

Electron Microscopy Studies of Ternary Diluted Magnetic Compounds Obtained by Chemical Vapor Transport Methods

Dwight R. Acosta¹ and Felipe Rábago²

¹ Instituto de Física, U.N.A.M., A.P. 20-364, 01000 México D.F. Fax: 525-616-1535

² Instituto de Física, U.A.S.L.P., Av. Obregón 64, San Luis Potosí, México.

ABSTRACT

Semiconductor compounds whose lattice is made up in part of substitutional magnetic ions, have received a great deal of attention in the last decade due to its interesting semiconducting and structural properties. As diluted magnetic semiconductors (DMS) their magnetic properties make them relevant for opto-electronic uses. In this work we present an electron microscopy study of the ternary compounds: $Cd_{0.95}Mn_{0.05}Se$ and $Cd_{0.9}Mn_{0.1}Te$, that were prepared by Chemical Vapor Transport methods. Samples were observed by Scanning Electron Microscopy (SEM), Conventional and High Resolution Electron Microscopy (CTEM and HREM respectively).

Characteristics of the growth of the bulk material were observed and structural details that might be related with the stability of ternary phases were derived.

KEY WORDS

Diluted magnetic semiconductors, electron microscopy, chemical vapor transport.

INTRODUCTION

The ternary compounds studied in this work belong to the so called Diluted Magnetic Semiconductors (DMS), also known like semi-magnetic semiconductors. In these materials a fraction of the atoms of the group II is replaced at random by manganese. Among several reasons to study these compounds, for us, an attractive one, is that the substitutional Mn atoms in II-VI compounds give highly efficient electroluminescence, very interesting for optical flat panel display [1]. Also the possibility to change the lattice constant and band parameters in function of Mn concentration, good for quantum wells and superstructures is present with the substitutions. The two crystal structures in which the $A^{II}_{1-x}Mn_xB^{VI}$ compounds are commonly formed - zinc blende and wurzite, shown in figures 1 and 2 respectively - are closely related, but with differences in symmetry properties.

EXPERIMENTAL

Sample Preparation and Observations

Start materials for DMS alloys are the binary $A^{II}B^{VI}$ and MnB^{VI} compounds. Single crystals [2] were obtained using the Chemical Vapor Transport (CVT) [3] [4] technique. For our case iodine was used like transport agent in the amount of 10 mg/cm^3 of the ampoule volume. Ampoule was placed in an horizontal furnace for a week at around 950°C . Small crystals but good quality were obtained. SEM observations were carried out in JEOL 5200 microscope and CTEM and HREM observations were carried out in a JEOL 4000 EX equipped with a high resolution pole piece ($C_s = 1.00 \text{ mm}$). For SEM studies small pieces (around 0.3 mm in size) were mounted directly on the holder. For HREM observations, samples did not receive special thinning treatment: Small grains were cracked and ground softly in an agata mortar; then the fine powder was sprayed, in each case, on 200 mesh copper grids covered with carbon holey film. HREM images were obtained from the thin border of very small grains.

RESULTS

Figure 3 is a SEM image from $\text{Cd}_{0.95}\text{Mn}_{0.05}\text{Se}$ (Se-DMS) where laminate configurations can be observed. The piling up of laminates is visible at least in two apparently perpendicular orientations, marked with arrows. The spacing between laminate looks different in each case. The terminal walls of laminate structures look clean and without roughness details. Figure 4 is other SEM image of Se-DMS, where piled up bent planes or laminates together with fractures in transverse direction to the laminate planes can be observed. Figure 5 is a Selected Area Electron Diffraction (SAED) pattern, from which crystallographic and structural details were derived for Se-DMS material; streaks between diffractions spots are also visible in the image. Figure 6 is a SAED pattern, from Te-DMS material, where together with crystallographic details, streaks coming from structural defects can be observed. Figure 7 is a HREM image from Se-DMS; two neighbouring and high ordered grains without a clear boundary between them can be appreciated. In Figure 8 another HREM image from Se DMS material coming from a zone close to the border of a laminate configuration is presented. Neighbouring crystallites with different orientations marked with A and B and pinholes marked with C are visible. Figure 9 is a SEM image of $\text{Cd}_{0.9}\text{Mn}_{0.1}\text{Te}$ (Te-DMS) sample. Laminate configurations with a great number of terraces with clean surfaces are observed. In Figure 10 the piling up of laminates is also observed in which seems to be the border of terraces. Figures 11 and 12 are HREM images of Te-DMS; twins and stacking faults together with perfect structures are visible in Figure 11 while polytype configurations and which seems to be an amorphous zone can be observed in Figure 12.

DISCUSSION AND CONCLUSIONS

Diluted Magnetic Semiconductor materials: Se-DMS and Te-DMS, have been successfully prepared using Chemical Vapor Transport methods. Identification for each ternary compound, was obtained from SAED patterns analysis. Crystallographic hexagonal and cubic structures for Se-DMS and Te-DMS respectively were clearly detected from the geometry and parameters derived from several SAED patterns, but a full correspondence with the lattice interplanar distances set, was not obtained for the two ternary compounds. Variations in lattices distances detected, correspond to d_{100} and d_{110} for Se-DMS and d_{111} and d_{311} for Te-DMS material. The local variations

detected in lattice parameters might be associated with the presence of a second precipitated phase in each case or with the mismatch due to the interpenetration of fcc sublattices in wurzite structure for Se-DMS compound and in the hcp sublattices in Te-DMS compound. The physical cause for the mismatch also could be local variations in the Mn concentration during the growth process, which can induce phase transitions in DMS materials [5]. The layered configurations in specific orientations observed in SEM images seem to be a predominant characteristic in DMS materials obtained by chemical transport methods and might be connected with directional bonding [6] among the ternary atoms in each structure. The cleanliness observed in some faces of crystallites could be related with the intriguing [7] elastic properties observed in DMS materials. HREM images from Se-DMS compounds reveal a high ordered material with a low density of structural defects and the absence of significative number of superlattices in the structure is noticeable in HREM images; this is not an intrinsic property in the materials and has to do with the directions available for observations in the crystallites. HREM images from Te-DMS samples reveal the presence of a relative low number of structural defects like dislocations, twinings and stacking faults that could have to do with c/a ratio variations in hexagonal structures [8]. Also polytype and superlattice structures were detected in this material from SAED patterns and HREM images but full characterization of this structures is not concluded. The structural disorders detected in our samples seem not to be a consequence of diffusion on Mn atoms inside the Cd Se and Cd Te lattices during the CVT processes and the deviations from lattice parameters do not give information about size and quantity of Mn^{2+} magnetic ions localized in each DMS lattice. Imperfections in DMS crystallographic structures might lead to anisotropy in magnetic properties [9].

ACKNOWLEDGEMENTS

Technical assistance of Mr. Luis Rendón and Ms. Jacqueline Cañetas in high resolution electron microscopy and scanning electron microscopy works, respectively are here recognized.

WURTZITE STRUCTURE

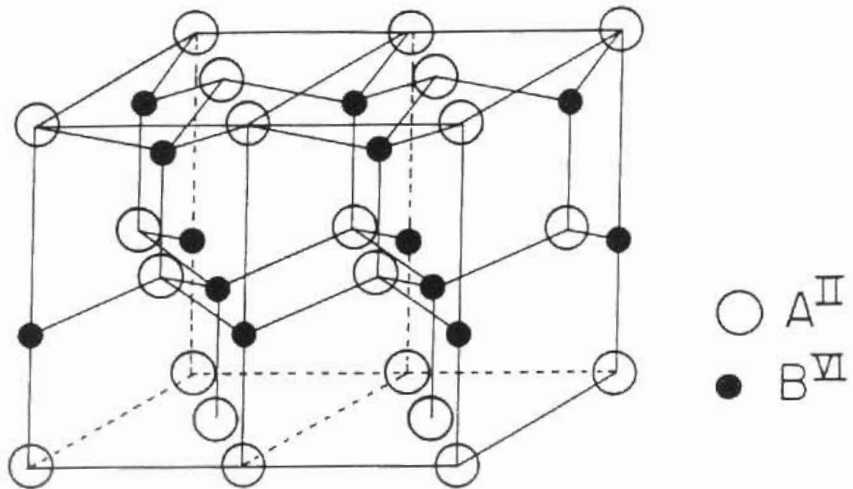


Fig. 1 Structure associated to $\text{Cd}_{1-x} \text{Mn}_x \text{Se}$,
DMS compound.

ZINC BLENDE STRUCTURE

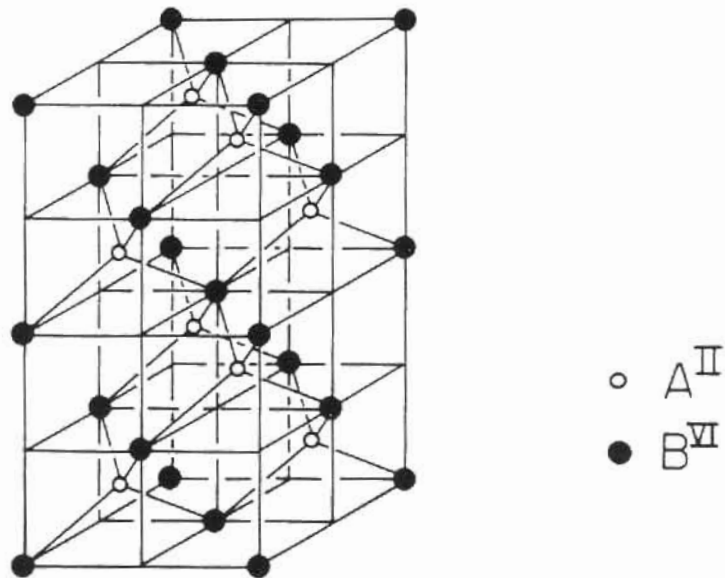


Fig. 2 Structure associated to $\text{Cd}_{1-x} \text{Mn}_x \text{Te}$,
DMS compound.

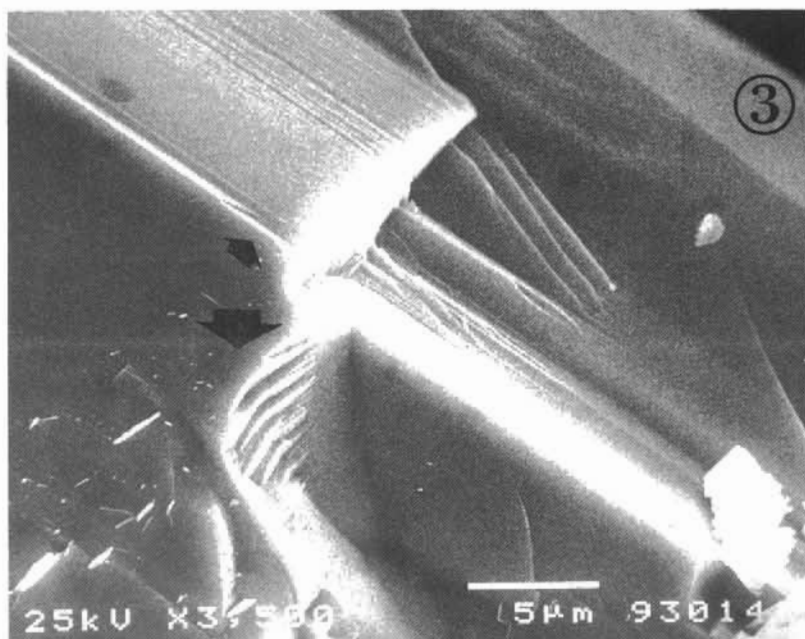


Fig. 3 Scanning Electron Microscope image of Se-DMS. Layered configurations in two different directions and cleanliness on surfaces can be appreciated.

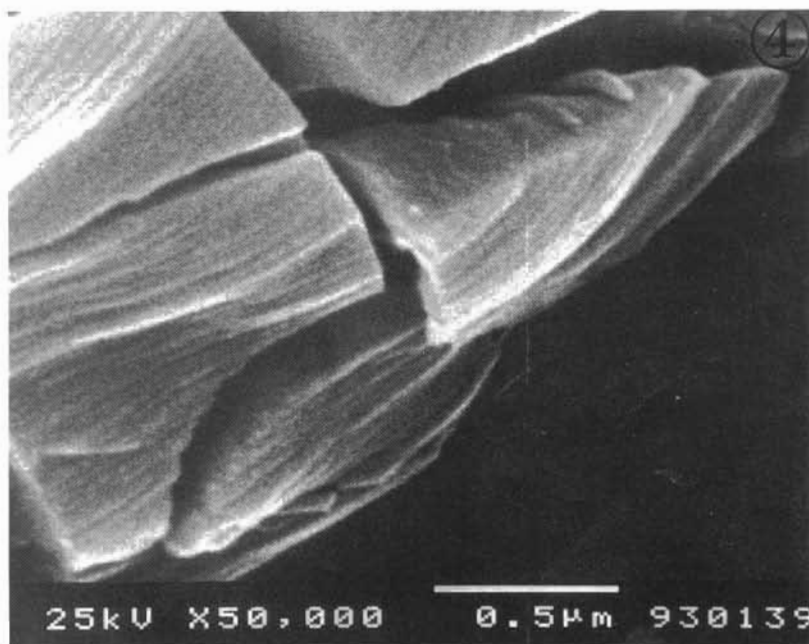


Fig. 4 In this SEM micrograph the piling up of bent planes with perpendicular cracks to Se-DMS planes are clearly identified.

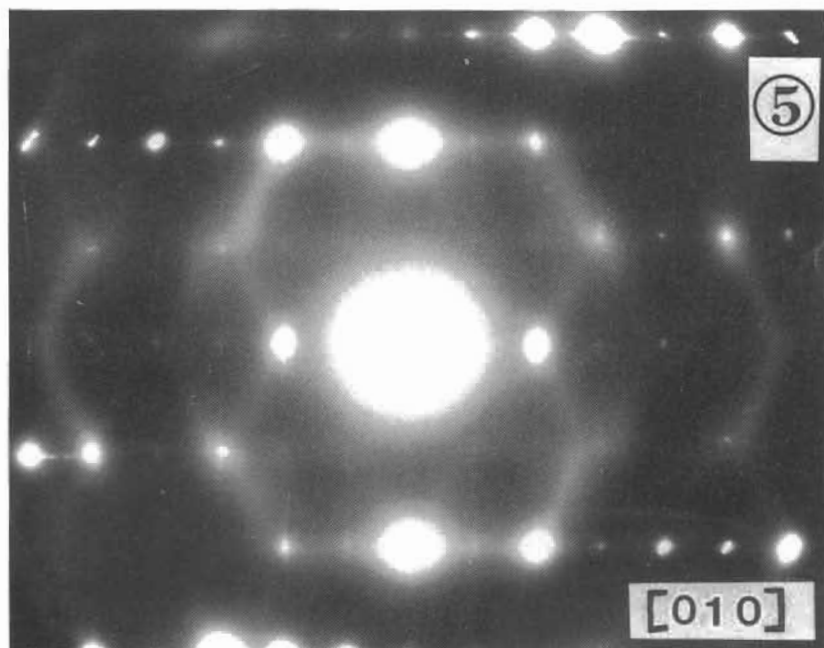


Fig. 5 Selected Area Electron Diffraction pattern from the border of a Se-DMS big grain and from which, Wurzite structure was derived.

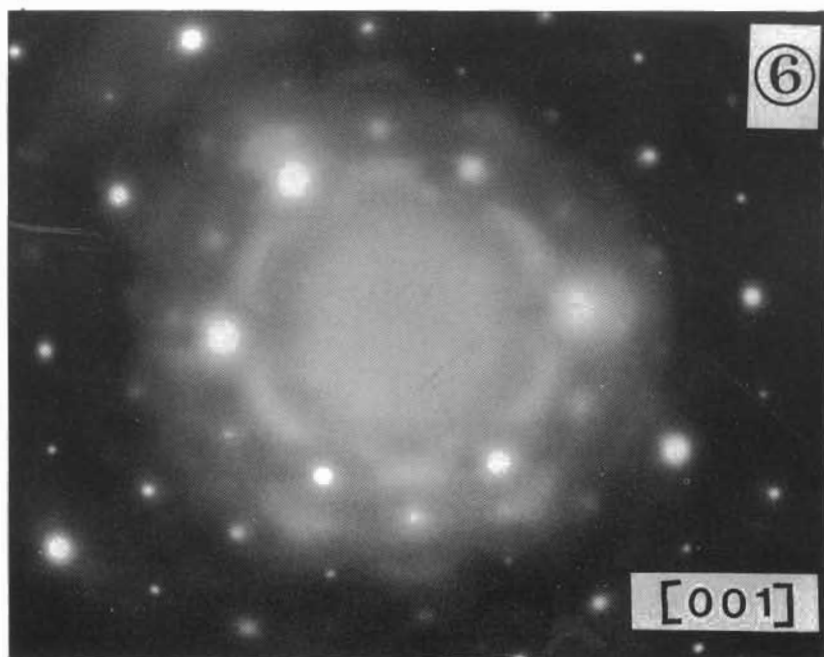


Fig. 6 Selected Area Electron Diffraction pattern from Te-DMS material. Diffuse streaks coming from geometrical effects are visible.

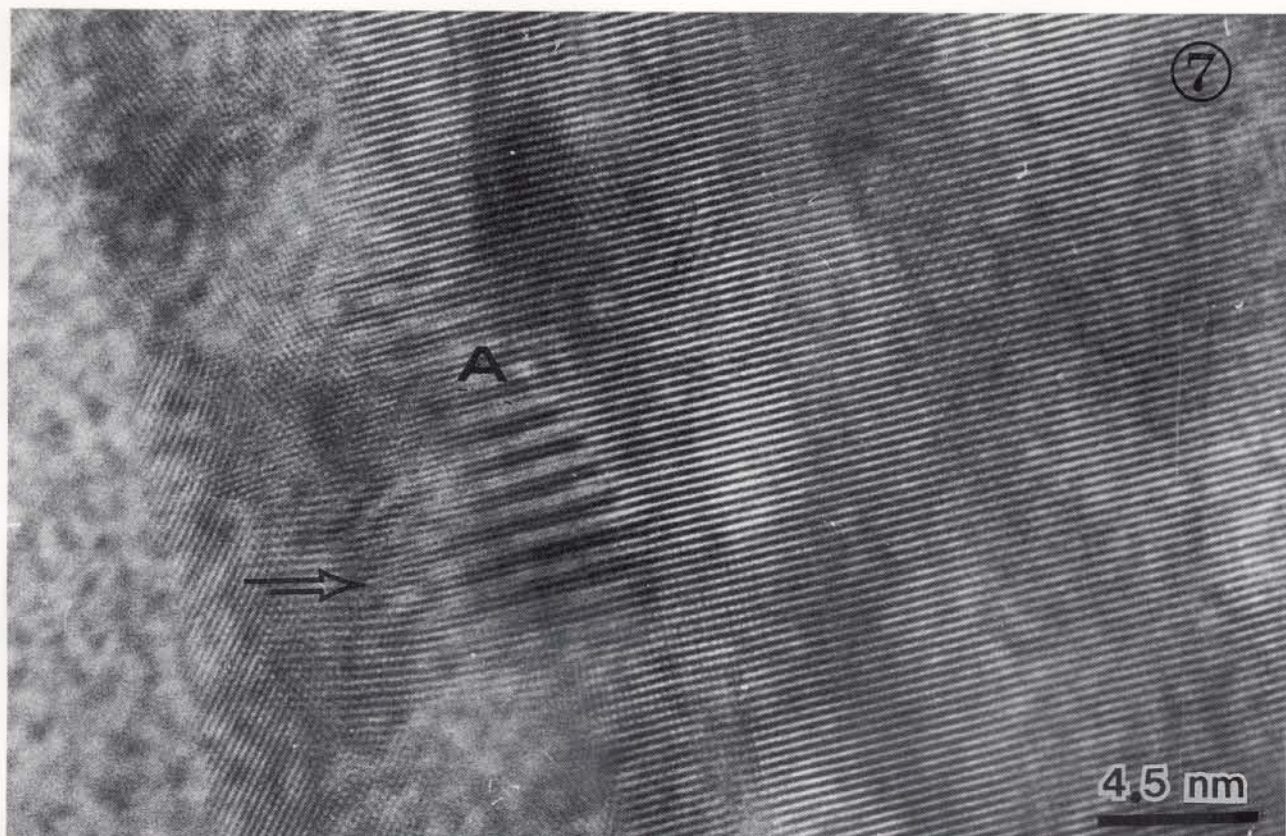


Fig. 7 High Resolution Electron Micrograph from Se-DMS. Superlattice configurations marked with A and arrowed dislocations are visible in the left side of the picture.

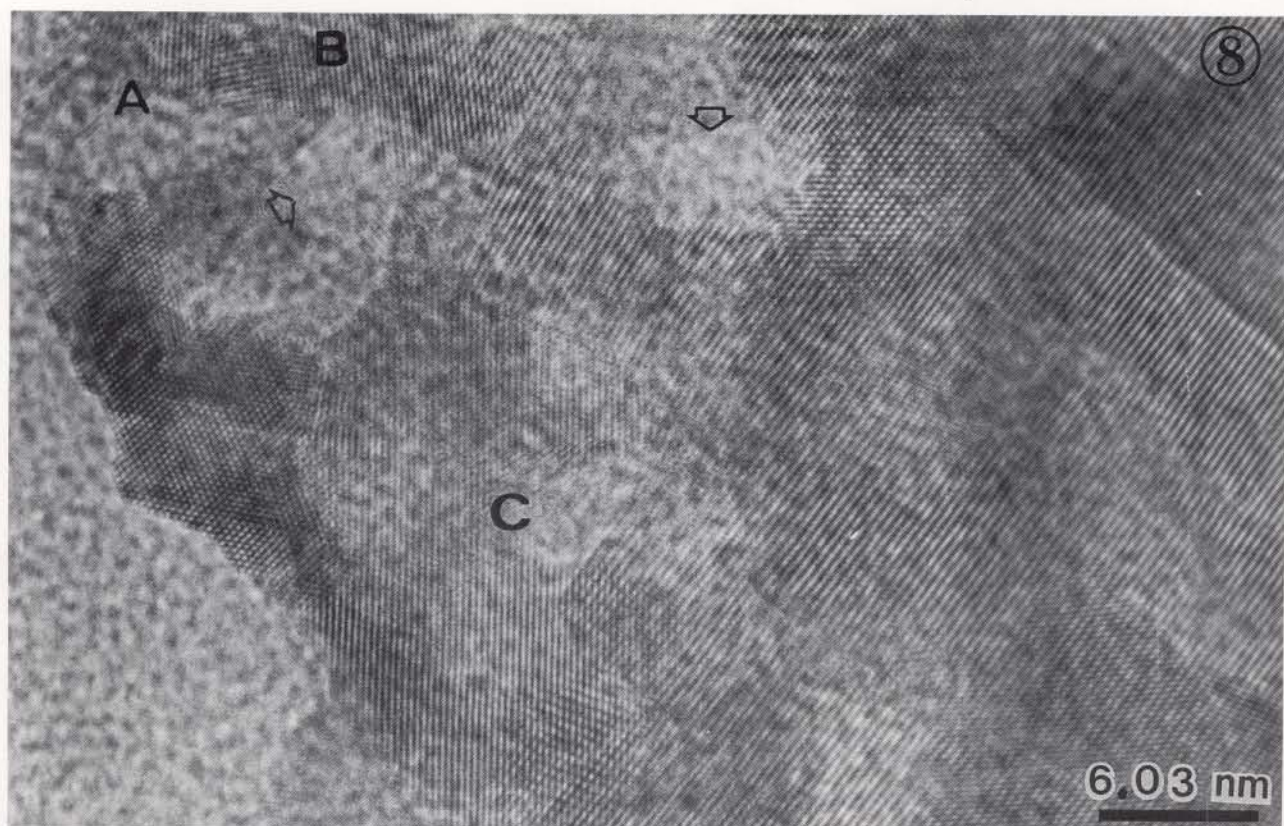


Fig. 8 High resolution image of Se-DMS from the border of a grain. Pinholes arrowed and highly ordered material can be observed in the picture.

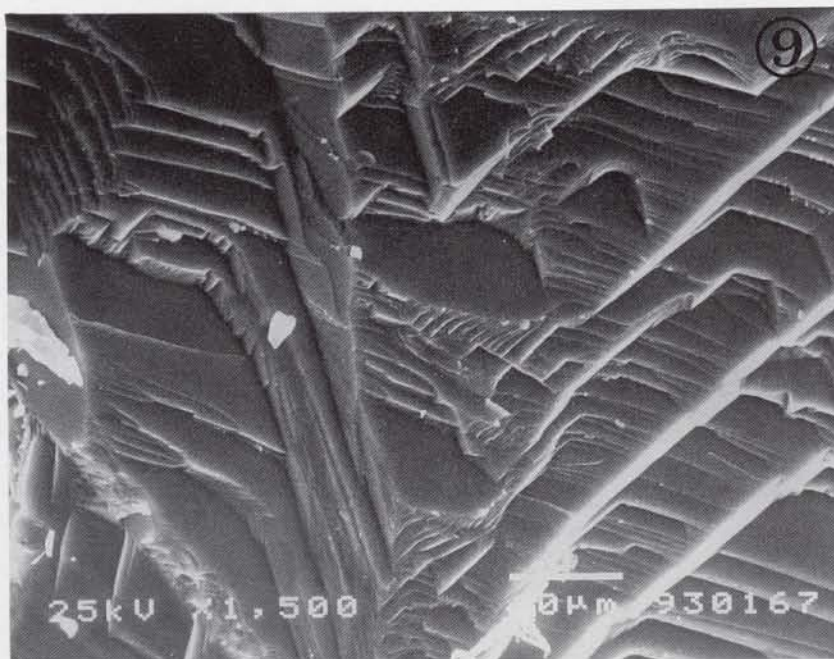


Fig. 9 Scanning Electron Microscope image from a border of a Te-DMS grain. Clean terraces and layered configurations are typical in this sample.

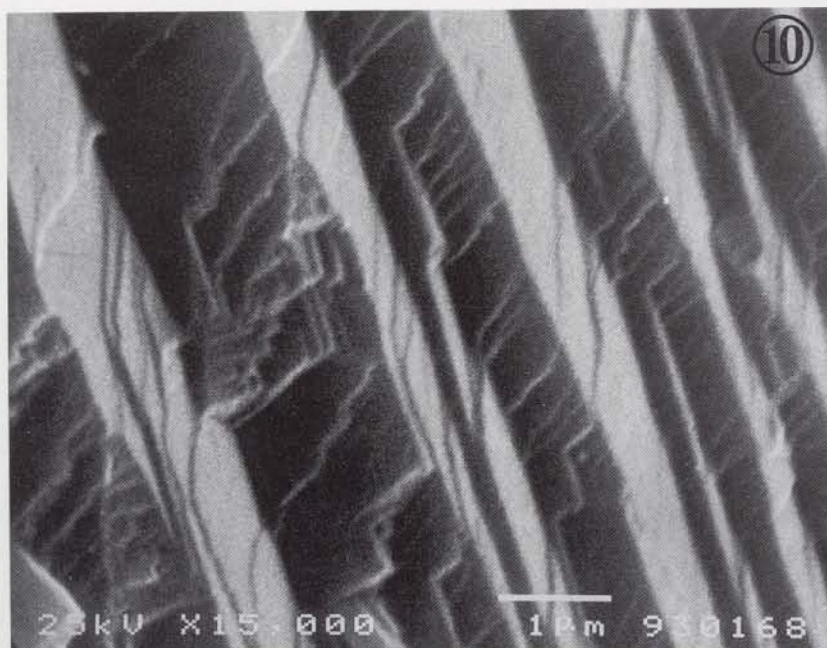


Fig. 10 Clean surfaces and layered configurations in at least two directions are visible in this SEM image coming from another grain of Te-DMS material.

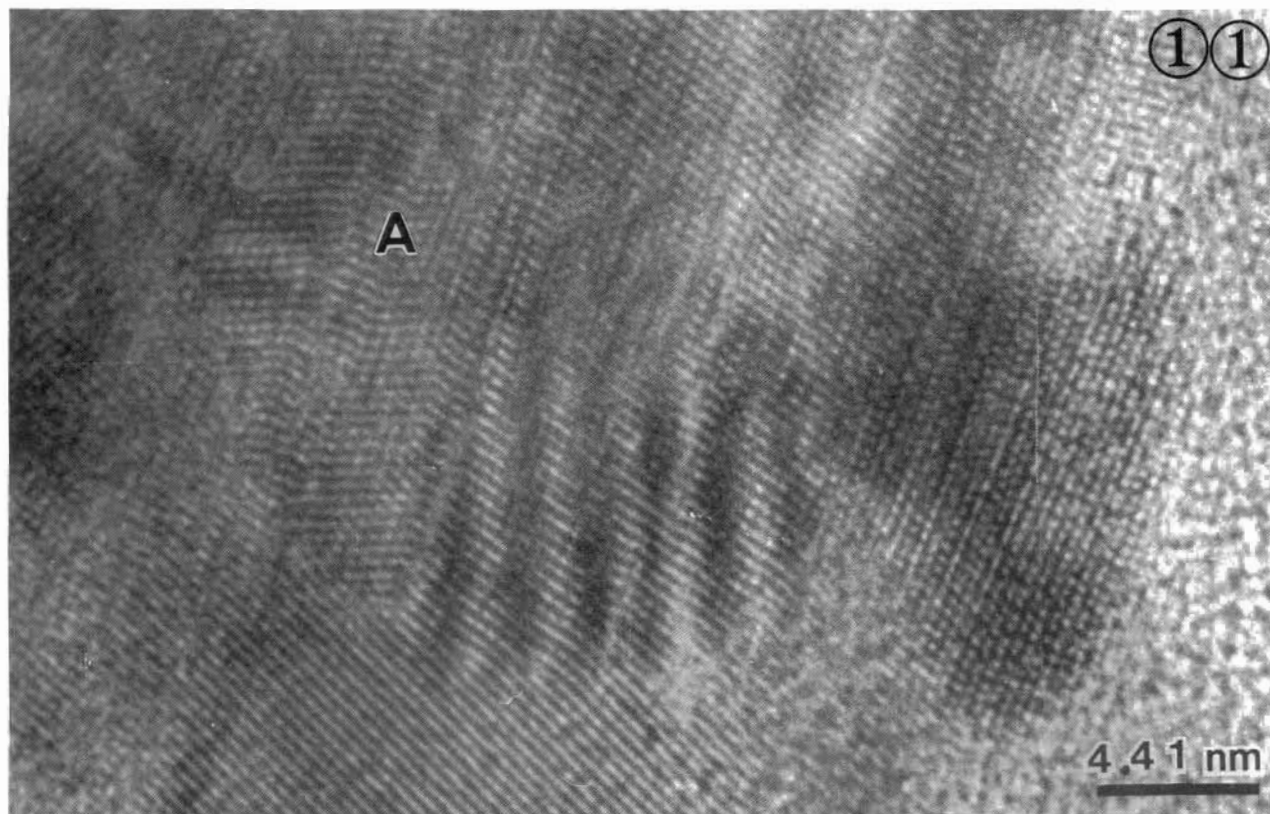


Fig. 11 High Resolution Electron Microscope image from Te-DMS. Twinned zone marked with A and dislocations in the central lower zone and Moiré fringes can be observed.

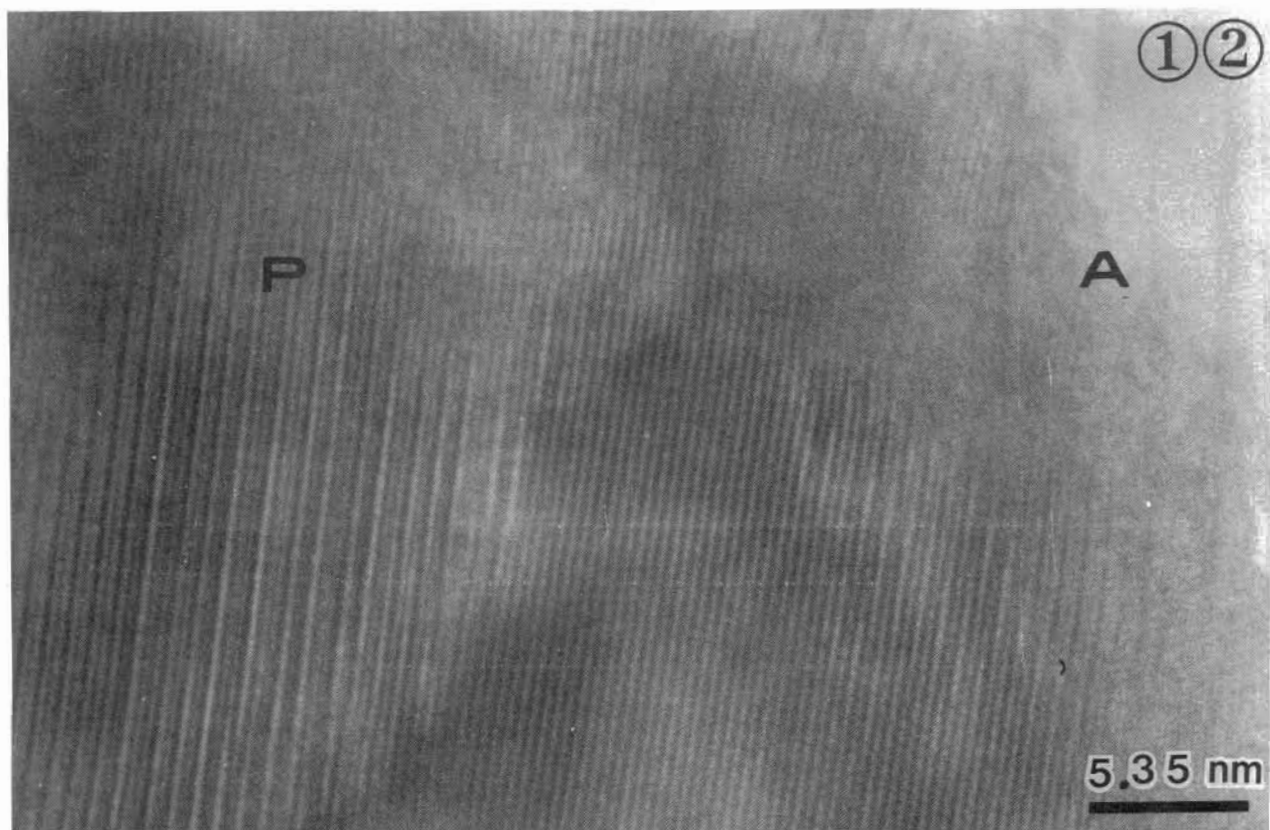


Fig. 12 High Resolution Electron Micrograph of Te-DMS. Polytype configurations and an amorphous zone marked with A are visible in the image.

RESUMEN

En la última década los materiales semiconductores compuestos cuya red está integrada parcialmente por iones magnéticos sustitucionales han recibido mucha atención debido a sus interesantes propiedades estructurales y semiconductoras. Como semiconductores magnéticos diluidos (DMS), sus propiedades magnéticas los hacen relevantes para usos optoelectrónicos. En nuestro trabajo realizamos un estudio por microscopía electrónica de los compuestos ternarios: $Cd_{0.95}Mn_{0.05}Se$ y $Cd_{0.9}Mn_{0.1}Te$, que fueron obtenidos por Transporte Químico en Fase Vapor (CVD). Las muestras fueron observadas por microscopía electrónica de barrido (SEM), microscopía electrónica convencional y de alta resolución (CTEM y HREM respectivamente). Características del crecimiento volumétrico del material fueron observadas y se detectaron detalles de las estructuras que pueden estar relacionados con la estabilidad de las fases ternarias obtenidas.

9. Steinberger, U., Lebeck, B. and Galazka, R.R. (1986) Neutron scattering studies of a dilute magnetic semiconductor $Cd_{1-x}Mn_xTe$. *J. Magn. Magn.* **54-57**: 1285.

REFERENCES

1. Furdyna, J.K., (1988) Diluted Magnetic Semiconductors. *J. Appl. Phys.* **64**: R29.
2. Samples prepared at the Instituto Venezolano de Investigaciones Científicas by one of authors (FR) with Dr. W. Giriat.
3. Triboulet, R., Rabago, F., Legros, R. and Lozykowsky, H. (1982) Low Temperature Growth of ZnSe Crystals. *J. Cryst. Growth*, **59**: 127.
4. Kaldis, E. (1965) Nucleation and Growth of Single Crystal by Chemical Transport II: Zinc Selenide. *J. Phys. Chem. Sol.*, **26**: 1701.
5. Giriat, W. and Furdyna, J.K. (1988) Semiconductors and semimetals, (ed. J. Furdyna and J. Kossut), Acad. Press, Vol. **25**: pp 1-34.
6. Yoder, D.R., Desk, U. and Furdyna, J.K. (1985) Lattice parameters of $Zn_{1-x}Mn_xSe$ and tetrahedral bonds lengths and $A^{II}_{1-x}N_xB^{VI}$. *J. Appl. Phys.* **58**: 4056.
7. Wu, A.Y. and Sladek, R.J. (1981) Ultrasonic phonon velocities in $Cd_{1-x}Mn_xTe$ Between 1.5 and 96 anomalies near the magnetic transition. *J. Phys.(Paris) Colloq.* **42**: C6-646.
8. Wu, A.Y. and Sladek, R.J. (1982) Imperfections in the crystal structure of $Cd_{1-x}Mn_xTe$. *J. Appl. Phys.* **53**: 8589-8492.